Spatio-Temporal Dynamics of Citrus Variegated Chlorosis: A Preliminary Analysis

F. F. Laranjeira, T. R. Gottwald, L. Amorim, R. D. Berger, and A. Bergamin Filho

ABSTRACT. The temporal and spatial dynamics of citrus variegated chlorosis (CVC), caused by *Xylella fastidiosa*, were examined for each of three citrus plots with 630, 3,960, and 1,440 trees, respectively, in the northern region of São Paulo State, Brazil. The progress of CVC, assessed bimonthly for over 2 yr, was best expressed as a double-sigmoid curve for each of the three plots. These curves were best fitted by non-linear regression to a generalized logistic function with five parameters, $y_t = p1/(1 + \exp(-(p_2 + p_3t + p_4t_2 + p_5t_3)))$, where y_t was disease incidence, t was time, and p_1 to p_5 were equation parameters. The final disease proportion in the three plots ranged from 0.14 to 0.98. Ordinary-runs analysis indicated some within-row aggregation of CVC-diseased trees for two of the three plots studied and some across-row aggregation of CVC-diseased trees for one of the plots where a distinct edge effect was noted. Dispersion indices calculated as (v_{obs}/v_{bin}), used as a general indicator of spatial dependency within the test plots, indicated a high degree of aggregation in one plot, and slight aggregation in the other two plots. When the binary form of Taylor's power law equation was used to analyze spatial dependency over time, significant aggregation of trees with CVC was indicated only for one plot when the quadrat size was 4×4 trees.

Citrus variegated chlorosis (CVC) was first discovered in 1987 (17), in the municipality of Colina, State of São Paulo, Brazil. This disease subsequently has become the most important disease problem for Brazilian citriculture. CVC causes an estimated yearly loss around US$100 million (8). Since 1990, much has been done to identify and characterize the cause of the problem, and develop rational and economical control methods for the disease. Three years after its first detection, the expression of CVC symptoms was associated with the constant presence of *Xylella fastidiosa* in the xylem of diseased plants (17). The pathogenicity of the bacteria was confirmed by the completion of Koch's postulates (3, 6). Identification of sharpshooters (e.g., *Acrogonia* sp., *Dilobopterus costalimai*, *Oncometopia facialis*, and other species) as vectors of the pathogen was then clarified (9, 16). These research findings presented opportunities for studies of the disease dynamics. During this same period, specific molecular tools for detection of *X. fastidiosa* were developed (1, 4, 14).

In contrast to the rapid progress of research to identify *X. fastidiosa* as the causal agent of CVC including its molecular characterization, epidemiological research had received little attention. The only papers on the epidemiology of CVC were the preliminary analysis by Gottwald et al. (5), the spatial analysis of one grove by Nelson (13), and the contribution of Laranjeira (8). These papers left no doubt that the *X. fastidiosa*-citrus pathosystem had its own unique characteristics. The conclusions inferred from the knowledge of other pathosystems involving *Xylella*, such as Pierce's disease of grapevine and phony peach disease (15) did not seem to apply to citrus.

The objective of this study was to examine the temporal and spatial dynamics for the incidence of CVC from three outbreaks of the disease.

MATERIALS AND METHODS

The incidence and spatial position of CVC-affected trees were recorded bimonthly from September 1994 to March 1996 in three plots on the São José farm near Bebedouro in São Paulo State. Plot 1 had 2,880 trees of Pera sweet orange on Rangpur lime rootstock in 18

east-west rows planted on a 8m × 3m pattern. This plot was bordered by Natal sweet orange trees planted in 1993 on the east, old orange trees on the west, and by Plot 2 on the south. The eastern 22% (720 trees) of Plot 1 were used in these analyses. Plot 2 had 3,960 trees of Pera sweet orange on Rangpur lime rootstock in 33 east-west rows planted on a 8m × 4m pattern. Plot 2 was bordered by Plot 1 on the north, Pera sweet orange planted in 1993 on the south, Natal sweet orange trees planted in 1993 on the east, and older planting of Pera orange trees on the west. The eastern 47.5% (1881 trees) were used for analyses. Plot 3 had 1,440 trees of Natal sweet orange on Rangpur lime rootstock in 18 east-west rows planted on a 7.5m × 4.5m pattern. Plot 3 was bordered by Natal sweet orange trees planted in 1993 on the north and Pera sweet orange planted in 1993 on the west, and corn (in 1994-1995) and soybean (in 1995-1996) on the south and east. Disease incidence for each tree in the plots was recorded as presence or absence of symptoms, based on the bimonthly visual assessments over a 26-mo period.

To characterize the temporal dynamics of CVC over 2 yr, a generalization of three functions (logistic, Gompertz, and monomolecular) modified for double-sigmoid curves (7) each with either four or five parameters, p, were fit to the incidences for each plot over time. The six functions tested were: i) logistic with four parameters, L4, [$y_t = p_1/(1 + \exp- (p_2 + p_3t + p_4t^2 + p_42t^3/3p_3))$]; ii) logistic with five parameters, L5, [$y_t = p_1/(1 + \exp (- (p_2 + p_3t + p_4t^2 + p_5t^3)))$]; iii) Gompertz with four parameters, G4, [$y_t = p_1(\exp (-\exp (- (p_2 + p_3t + p_4t^2 + p_42t^3/3p_3))))$]; iv) Gompertz with five parameters, G5, [$y_t = p_1 (\exp (-\exp (- (p_2 + p_3t + p_4t^2 + p_5t^3)))))$]; v) monomolecular with four parameters, M4, [$y_t = p_1(1-\exp (- (p_2 + p_3t + p_4t^2 + p_42t^3/3p_3)))$]; and vi) monomolecular with five parameters, M5, [$y_t = p_1(1-\exp (-(p_2 + p_3t + p_4t^2 + p_5t^3)))$]; where y was the disease incidence (proportion of diseased trees), t was time (months), p_1 represented the upper asymptote, p_2 was related to the initial disease level y_0 (value of y when time was 0), and p_3, p_4, and p_5 were parameters that described the infection rate, variable in time (7). These models were fitted to disease incidence of each plot by nonlinear-regression analysis (iteration method) using the software STATISTICA (Statsoft, Tulsa, OK). The appropriateness of each model was assessed by correlation of the observed versus predicted values and examination of the residuals of regression for patterns which would indicate an inappropriate fit of the model (2).

Three approaches were used to characterize the spatial dynamics of CVC. First, the aggregation of diseased trees within rows was tested by ordinary runs analysis for each plot on each assessment date (12). Results were reported as the number of rows with significantly (P = 0.05) fewer runs than expected (i.e., aggregation). Second, to detect the presence of aggregation at different spatial scales, each plot on each assessment date was divided into 2 × 2-, 3 × 3-, and 4 × 4-tree quadrats, starting at the northeast corner of each plot. The spatial distribution of quadrats with CVC-diseased trees was analyzed for each of the three sizes of quadrats by the index of dispersion (D), calculated as the ratio of observed to binomial variance (10). Finally, to examine the trends in aggregation over time, the binary form of Taylor's power law was used. This was expressed as $\log (v_{obs}) = \log (A) + b \log (v_{bin})$, in which v_{obs} was the observed variance, v_{bin} was the theoretical variance of the proportion of diseased trees for a binomial (random) distribution, and A and b were linear regression parameters (10, 11). This equation was fit to the

variances for the ten assessment dates of each plot, for each of the three quadrat sizes. Significance of A and b (A and b >1) was determined by t-test.

RESULTS AND DISCUSSION

Disease incidence over time. For the 2 yr period of disease assessment, the two nonlinear functions which were the most appropriate to describe the increase in incidence of CVC over time were the generalization of the logistic function and the Gompertz function, both with five parameters (Table 1). Both models had high correlation coefficients of determination (R^2) of observed versus predicted values and no patterns were observed in the graphs of residuals for the three plots. For some of the models the estimated values of p_1 were unrealistically high because the observed data did not show a clear asymptotic phase (Fig. 1). The logistic function gave the best estimate for the upper asymptote (p_1). The maximum observed disease incidence (March 1996) was 88% in Plot 1, 98% in Plot 2, and 14% in Plot 3 (Fig. 1). In all plots, the disease progress showed a clear, double-sigmoid pattern, with two distinct periods of disease increase between September and March (spring and summer in Brazil) and plateaus during which disease increase was less pronounced in the fall and winter between the two years. The curve shapes that we found for our bimonthly assessments were quite different from the simple, Gompertz-shaped curves shown previously (5) for the annual progress of CVC. Obviously, the

TABLE 1
COEFFICIENTS OF DETERMINATION (R^2), UPPER ASYMPTOTE ESTIMATE (P_1), AND PRESENCE OF PATTERNS IN THE STANDARD RESIDUAL PLOTS (RP) DETERMINED BY NONLINEAR REGRESSION ANALYSIS OF DISEASE INCIDENCE OF CITRUS VARIEGATED CHLOROSIS

Plot	Model[z]	Obs. ymax	R^{2y}	p_1X	RP[w]
1	L4	0.88	0.965	2.21	-
2	L4	0.98	0.975	18.06	-
3	L4	0.14	0.917	202.02	+
1	L5	0.88	0.996	0.91	-
2	L5	0.98	0.989	1.00	-
3	L5	0.14	0.988	0.19	-
1	G4	0.88	0.993	0.93	-
2	G4	0.98	0.976	7.72	-
3	G4	0.14	0.935	0.13	-
1	G5	0.88	0.994	0.97	-
2	G5	0.98	0.985	1.06	-
3	G5	0.14	0.992	0.31	-
1	M4	0.88	0.979	2,012.90	+
2	M4	0.98	0.977	137.24	+
3	M4	0.14	0.916	1,102.90	+
1	M5	0.88	0.988	11.93	+
2	M5	0.98	0.981	1.31	-
3	M5	0.14	0.992	3.55	-

[z]Functions of disease progress: generalization of the logistic function with 4 parameters, L4 or with 5 parameters, L5; generalization of the Gompertz function with 4 parameters, G4 or with 5 parameters, G5; generalization of the monomolecular function with 4 parameters, M4 or with 5 parameters, M5.
[y]Coefficients of determination of observed versus predicted values.
[x]Estimated upper asymptote (proportion).
[w]Presence (+) or absence (-) of patterns in the standard residual graphs.

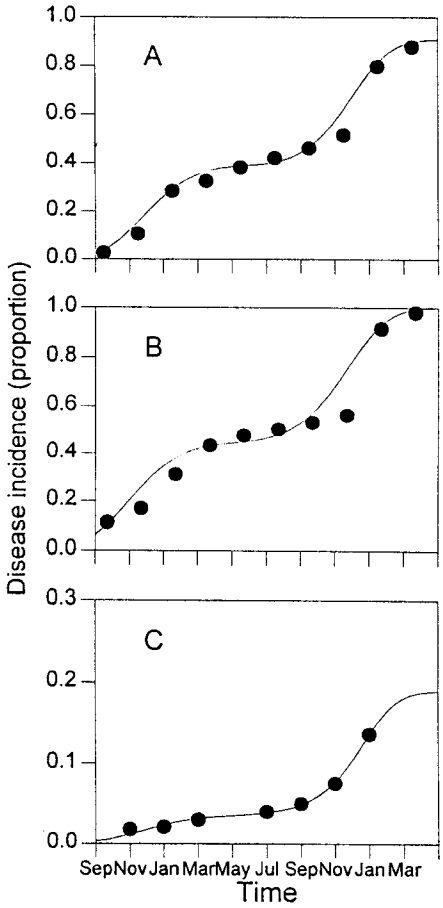

Fig. 1. Disease progress curves of CVC in Plots 1 (A), 2 (B), and 3 (C). Dots represent original data and the solid line represent the fitted curves.

within-year variation of increase in CVC that we found would not have been detected in the annual surveys used by Gottwald et al. (5). The double-sigmoid pattern was seen by conducting multiple assessments over a 2-yr period. In areas where the disease progresses more slowly, i.e., more southern citrus growing areas, CVC epidemics may require multiple years to reach an asymptote. In such situations, yearly sigmoid patterns of disease increase would be anticipated with spring and summer increases and fall and winter plateaus. Thus, more complex temporal models related to triple-sigmoid, quadruple-sigmoid, etc. patterns may be necessary to describe these slower epidemics.

Spatial analyses. With the ordinary runs analysis, aggregation was observed for only one of the 18 rows on the first assessment of Plot 1 when there was 2.8% incidence. For this plot, the number of rows with significant aggregation increased to 10 rows for the assessment made in May 1995 when there was 38.5% incidence. Thereafter, seven or eight rows with significant aggregation were found toward the conclusion of the study as the incidence increased to about 88% (Table 2). For Plot 1, aggregation across-rows was rare. Across-row aggregation was indicated in only one of the possible 39 across-row tests, and this was seen only when disease incidence exceeded 42% (Table 2). For Plot 2, aggregation within-row increased over time as demonstrated by an increase of seven to 12 of the 30 rows possible within-rows tests indicating a departure from randomness, over the period of September 1994 to March 1995. Similarly, several across-row tests also indicated a departure from randomness. During this time, the disease incidence increased from 11.4 to 43.5% (Table 2). From May to November 1995, aggregation was observed on 10 rows. On the last two assessment dates for Plot 2, no aggregation was detected by ordinary runs analysis because the incidence of the disease was higher than 92%. The distribution of diseased trees in Plot 3 was mostly random as only one of 18 within-rows tests demonstrated significant aggregation for most of the assessment dates and was even more rare for across-row tests with only one row demonstrating aggregation and only during the final two assessment dates (Table 2). The final incidence of CVC in Plot 3 was low (<14%, Table 2).

The dispersion index (D) was utilized as a general indicator of the intensity of spatial dependency.

TABLE 2
ORDINARY RUNS ANALYSIS OF CITRUS VARIEGATED CHLOROSIS

Date of assessment (mo/yr)	Plot no.	Disease incidence	Within rows[z]		Across rows[z]	
			No. nonrandom tests	Total no. tests	No. nonrandom tests	Total no. tests
09/94	1	2.8	1	9	0	15
11/94	1	10.6	0	18	0	29
01/95	1	28.6	5	18	0	39
03/95	1	32.9	8	18	0	39
05/95	1	38.5	10	18	0	39
07/95	1	42.4	8	18	1	39
09/95	1	46.5	7	18	1	39
11/95	1	51.9	7	18	0	39
01/96	1	79.9	8	18	0	39
03/96	1	87.9	8	18	1	39
09/94	2	11.4	7	33	8	57
11/94	2	16.9	7	33	3	57
01/95	2	31.2	6	33	7	57
03/95	2	43.5	12	33	7	57
05/95	2	47.8	10	33	5	57
07/95	2	50.4	10	33	7	57
09/95	2	53.3	8	33	5	57
11/95	2	56.5	10	33	1	57
01/96	2	91.6	0	33	7	57
03/96	2	98.0	n.d.	n.d.	n.d.	0
09/94	3	0	n.d.	n.d.	n.d.	0
11/94	3	0.02	0	1	0	1
01/95	3	1.8	1	6	0	22
03/95	3	2.1	1	9	0	23
05/95	3	2.9	1	13	0	33
07/95	3	3.3	1	13	0	41
09/95	3	3.9	1	15	0	43
11/95	3	5.0	1	17	0	55
01/96	3	7.6	2	18	1	66
03/96	3	13.6	3	18	1	68

[z]n.d. - not determined (when incidence was either 0.0 or >92%).

When D-values are significantly (P = 0.05) greater than 1, this is interpreted as aggregation of diseased trees, whereas if D = 1 a random distribution of the disease is indicated, and if D < 1, the spatial pattern is interpreted as uniform. In Plot 1, only two of 30 assessments (10 assessment dates × 3 quadrat sizes) had significant aggregation (Table 3 and Fig. 2). Because of the higher incidence of CVC in Plot 2, significant aggregation was indicated for all assessment dates and for all three quadrat sizes. In Plot 3, significant aggregation was indicated for 10 of 27 assessments (9 assessment dates × 3 quadrat sizes) despite the low incidence of disease (Table 3 and Fig. 2).

When the binary form of Taylor's power law equation was fitted to the variances of the incidence for the 10 assessment dates, only one slope (b = 1.16) of the linear regression line was found to be significantly greater than 1.0 indicating aggregation in the plot over time. This significant (P = 0.001) slope was for data parsed into 4 × 4 quadrats in Plot 3; the plot with the least amount of disease (Table 4). Three origins, parameter A in the equation, were also found to be significant (log(A) > 0.0) (Table 4).

TABLE 3
DISPERSION INDEX (D) OF CITRUS VARIEGATED CHLOROSIS OVERTIME FOR THREE QUADRAT SIZES OF CITRUS TREES

Plot	Quadrat size	Date of assessment (month/year) 09/94	11/94	01/95	03/95	05/95	07/95	09/95	11/95	01/96	03/96
1	2 × 2	1.03	1.02	1.03	0.99	1.01	1.02	1.07	1.07	1.21[z]	1.14
	3 × 3	1.26	0.84	1.13	1.29	1.13	1.22	1.19	1.39	1.26	1.02
	4 × 4	1.04	0.74	0.98	1.00	1.00	0.93	0.99	1.06	1.13	0.88
2	2 × 2	1.25[z]	1.23	1.18	1.20	1.21	1.23	1.22	1.18	1.06	n.d[y]
	3 × 3	1.74	1.59	1.43	1.36	1.35	1.31	1.34	1.22	1.20	n.d.
	4 × 4	2.16	1.94	1.49	1.67	1.68	1.62	1.61	1.53	1.25	n.d.
3	2 × 2	n.d.[y]	0.99	1.26	1.21	1.10	1.10	1.02	1.02	1.08	1.14
	3 × 3	n.d.	0.99	1.43	1.38	1.15	1.15	1.04	1.02	1.40	1.45
	4 × 4	n.d.	0.98	1.24	1.17	1.15	1.15	1.17	1.29	1.59	1.79

[z]Underlined values were significantly ($P = 0.05$) different from 1.0.
[y]n.d. - not determined due to very low or very high incidence.

Early in the epidemic of CVC in the plots of citrus, the pattern of disease was mostly random, single-tree "foci" with occasional doublets or triplets of diseased trees. This pattern of primarily single trees with CVC had been noted earlier (8, 13). When the sharpshooter vectors enter a grove, they settle on individual trees. Even when disturbed, they tend to return to the same tree. When the sharpshooters no longer find these trees to be a favorable habitat, they take flight and move to trees at some distance, apparently forsaking the nearest neighboring trees. Obviously, as the incidence of trees with CVC intensifies, fewer disease-free solitary trees are available and small clusters of diseased trees occur simply by probability (J. R. S. Lopes, Department of Entomology, University of São Paulo/ESALQ-personal communication).

Some edge effects were noted on the maps of the three plots. The southern border of Plot 1 was in common with the northern border of Plot 2. A noticeable gradient for incidence of CVC was found on the northern border of Plot 2. This gradient persisted for most of the later assessment dates. Most likely, the inoculum/vector source for this gradient was from the old grove that was removed prior to the replanting of this planting (Plot 1) and before the study was initiated. The later edge effect on the southern border of Plot 1 probably came from infective sharpshooters that migrated northward from the more diseased planting (Plot 2). There was a slight edge effect of more diseased trees along the southern border of Plot 3 also. Since the neighboring plot to the southern border of this grove was planted to corn or soybean, this may mean that these latter crops may have provided a reservoir for specific species of sharpshooter vectors that affected the edge of the plot more than the plot interior.

The spatial analyses by the three methods led to slightly different but concurring conclusions regarding the degree of aggregation. To fully comprehend the results of the various analyses, we must keep in mind the spatial scale at which the analyses were conducted. Let us first examine the individual tree scale. Ordinary runs analysis, led to the interpretation that within-row aggregation occurred in all three plots sometime during the 2 yr of the study and became more prevalent as disease incidence increased. Across-row aggregation was rare from Plots 1 and 3 but was common for Plot 2. This was because Plot 2 had a distinct edge effect with CVC occurring

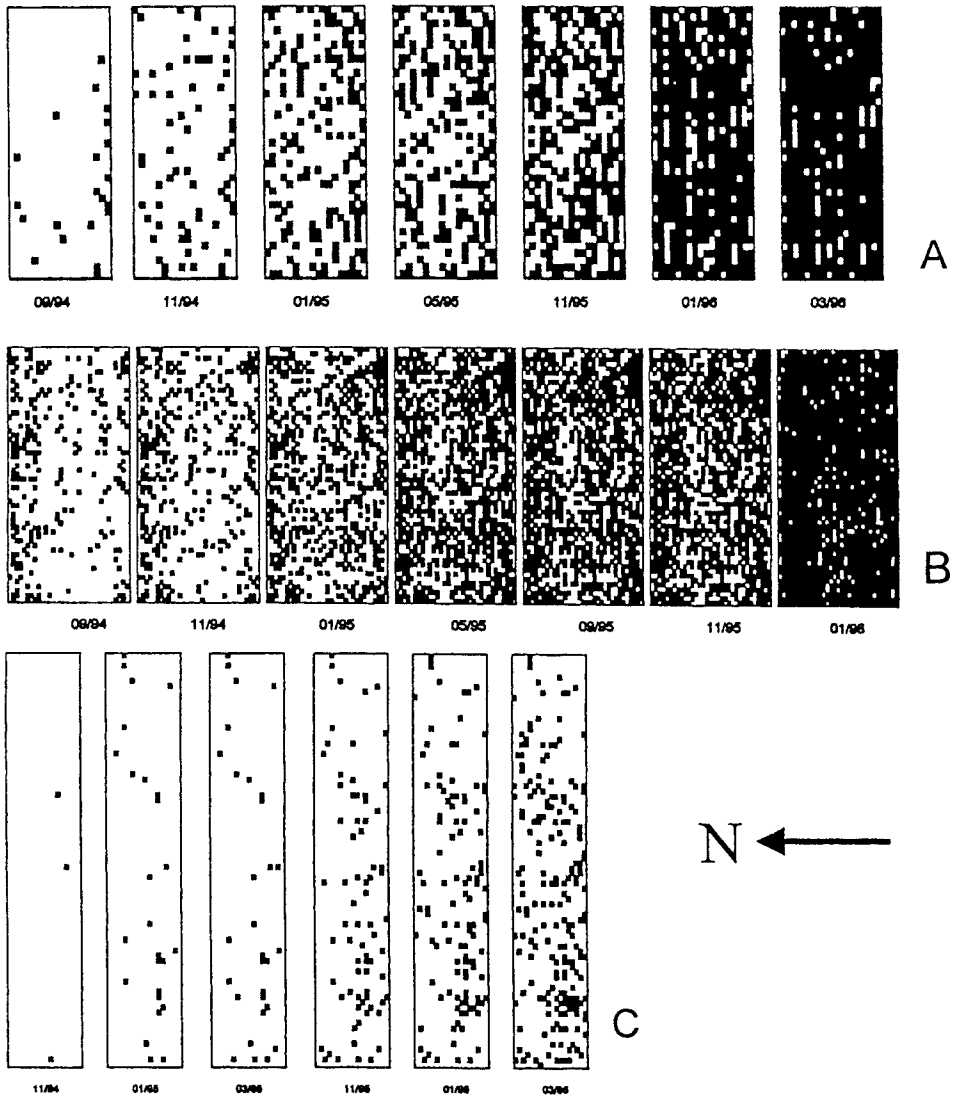

Fig. 2. Spatial pattern of diseased trees (black squares) in Plots 1 (A), 2 (B), and 3 (C) for different assessment dates.

more heavily along the first few rows on the northern border and thus contributed to a greater than expected number of across-row tests (Fig. 2). Similarly, Gottwald et al. (5) analyzed a single planting via ordinary runs and concluded that there was considerable clustering and spread from tree to neighboring tree. Analysis of foci is also conducted at the individual tree level. Nelson's analysis of foci of this same plot as previously analyzed by Gottwald et al. (5) provided further evidence that the epidemic began from predominantly isolated CVC-infected trees and foci of 1, 2, or 3 diseased trees dominated the overall pattern of incidence of CVC over the first few years (13). We also found that single, diseased trees dominated the pattern in the early epidemic, with aggregation being more common as the epidemic intensified.

Next we can examine the data at larger spatial dimensions, i.e., groups

TABLE 4
STATISTICAL SUMMARY FOR BINARY FORM OF TAYLOR'S POWER LAW EQUATION FIT TO THE INCIDENCE OF CITRUS VARIEGATED CHLOROSIS ON CITRUS TREES OVER TEN DATES OF ASSESSMENT

	Quadrat		Parameters of binary power law equation		
Plot	Size	Number	a = *log*(A)	b	R^2
1	2 × 2	153	0.019	0.99	0.991
	3 × 3	66	0.169	1.06	0.961
	4 × 4	32	0.030	1.02	0.980
2	2 × 2	448	0.166[y]	1.07	0.991
	3 × 3	209	0.091	0.97	0.915
	4 × 4	112	0.300	1.04	0.877
3	2 × 2	360	0.078	1.02	0.996
	3 × 3	156	0.246[z]	1.06	0.990
	4 × 4	80	0.556[x]	1.16[x]	0.992

[z]Significant at $P = 0.05$ according to t-test.
[y]Significant at $P = 0.01$ according to t-test.
[x]Significant at $P = 0.001$ according to t-test.

of trees from data parsed into 2 × 2, 3 × 3, or 4 × 4 quadrat sizes. For this larger spatial dimension the dispersion indices indicated rare aggregation and only for the final assessment dates for Plot 1, general aggregation for all quadrat sizes and assessment dates for Plot 2 and again rare aggregation for specific quadrat size and assessment date combinations for Plot 3. Gottwald et al. (5) also analyzed a single planting at this larger spatial dimension via spatial autocorrelation, and Morisita's Index of Dispersion, led them to conclude that there was considerable aggregation at the 'group' scale also. The analysis of Gottwald et al. (5) was therefore consistent with our analysis of Plot 2.

In contrast, the binary form of Taylor's power law equation, indicated only rare aggregation for specific quadrat sizes. Although this conclusion would seem to generally contradict index of dispersion and spatial autocorrelation analyses results, it does not. The dispersion index is calculated for specific assessment dates and represents the amount of aggregation that existed at a specific time, whereas, the Taylor's Power Law analyses is a spatio-temporal analysis and considers all assessment dates through time for a specific spatial dimension, i.e., quadrat size. Therefore, considering all of the individual assessment dates simultaneously, aggregation at the 'group' spatial dimension was not strongly indicated through time.

To date only four plots have been analyzed for the spatial and temporal dynamics of CVC, even when we consider Gottwald et al. (5) and Nelson's (13) previous work combined with the present study. These studies have clarified the characteristics of disease increase and spread to some extent. However, some indications of plot diversity are also indicated. A large number of vector species have been identified as capable of *X. fastidiosa* transmission within citrus, and the complement of vector species changes dynamically over time and by citrus-growing region. In addition, there are apparent differences in disease severity associated with different citrus regions within Brazil which may be associated with vector population complement and/or slight climatic differences. Intuitively, this combination of factors would likely lead to differing spatio-temporal dynamics among plots. Therefore, a much greater collection of data sets

from numerous plots and regions must be examined to more fully understand this serious disease. Unfortunately, CVC epidemics are polyetic (multi-year) in duration and, therefore, several years will be required to collect the necessary data to fully examine this disease.

LITERATURE CITED

1. Beretta, M. J. G., G. A. Barthe, T. L. Ceccardi, R. F. Lee, and K. S. Derrick
   1997. A survey for strains of *Xylella fastidiosa* in citrus affected by citrus variegated chlorosis and citrus blight in Brazil. Plant Dis. 81: 1196-1198.
2. Campbell, C. L. and L. V. Madden
   1990. Introduction to Plant Disease Epidemiology. Wiley, New York. 532 p.
3. Chang, C. J., M. Garnier, L. Zreik, V. Rossetti, and J. M. Bové
   1993. Culture and serological detection of the xylem-limited bacterium causing citrus variegated chlorosis and its identification as a strain of *Xylella fastidiosa*. Curr. Microbiol. 27: 137-142.
4. Garnier, M., C. J. Chang, L. Zreik, V. Rossetti, and J. M. Bové
   1993. Citrus variegated chlorosis: serological detection of *Xylella fastidiosa*, the bacterium associated with the disease. In: *Proc. 12th Conf. IOCV*, 301-305. IOCV, Riverside, CA.
5. Gottwald, T. R., F. B. Gidtti, J. M. Santos, and A. C. Carvalho
   1993. Preliminary spatial and temporal analysis of citrus variegated chlorosis (CVC) in São Paulo, Brazil. In: *Proc. 12th Conf. IOCV*, 327-335. IOCV, Riverside, CA.
6. Hartung, J. S., M. J. G. Beretta, R. H. Brlansky, J. Spisso, and R. F. Lee
   1994. Citrus variegated chlorosis bacterium: axenic culture, pathogenicity, and serological relationships with other strains of *Xylella fastidiosa*. Phytopathology 84: 591-597.
7. Hau, B., L. Amorim, and A. Bergamin Filho
   1993. Mathematical functions to describe disease progress curves of double sigmoid pattern. Phytopathology 83: 928-932.
8. Laranjeira, F. F.
   1997. Dinâmica Espacial e Temporal da Clorose Variegada dos Citros. Master Thesis, ESALQ, Piracicaba, Brazil. 144 p.
9. Lopes, J. R. S., M. J. G. Beretta, R. Harakawa, R. P. P. Almeida, R. Krügner, and A. Garcia Jr.
   1996. Confirmação da transmissão por cigarrinhas do agente causal da clorose variegada dos citros, *Xylella fastidiosa*. Fitopatol. Bras. 21: 343 (Abstr.).
10. Madden, L. V. and G. Hughes
    1995. Plant disease incidence: distributions, heterogeneity, and temporal analysis. Ann. Rev. Phytopathol. 33: 529-564.
11. Madden, L. V., G. Hughes, and M. A. Ellis
    1995. Spatial heterogeneity of the incidence of grape downy mildew. Phytopathology 85: 269-275.
12. Madden, L. V., R. Louie, J. J. Abt, and J. K. Knoke
    1982. Evaluation of tests for randomness of infected plants. Phytopathology 72: 195-198.
13. Nelson, S. C.
    1996. A simple analysis of disease foci. Phytopathology 86: 332-339.
14. Pooler, M. R. and J. S. Hartung
    1995. Specific PCR detection and identification of *Xylella fastidiosa* strains causing citrus variegated chlorosis. Curr. Microbiol. 31: 377-381.
15. Purcell, A.H. and D. L. Hopkins
    1996. Fastidious xylem-limited bacterial plant pathogens. Ann. Rev. Phytopathol. 34: 131-151.
16. Roberto, S. R., A. Coutinho, J. E. O. Lima, V. S. Miranda, and E. F. Carlos
    1996. Transmissão de *Xylella fastidiosa* pelas cigarrinhas *Dilobopterus costalimai, Acrogonia terminalis e Oncometopia facialis* (Hemiptera: Cicadellidae) em citros. Fitopatol. Bras. 21: 517-518.
17. Rossetti, V., M. Garnier, J. M. Bové, M. J. G. Beretta, A. R. Teixeira, J. A. Quaggio, and J. D. de Negri
    1990. Présence de bactéries dans le xylème d'orangers atteints de chlorose variegée, une nouvelle maladie des agrumes au Brésil. C.R. Acad. Sci. Paris Ser.III 310: 345-349.